Photosensitivity in Smith-Lemli-Opitz syndrome: A flux balance analysis of altered metabolism

Bell Raj Eapen*

Kaya Skin Clinic, Dubai, UAE; Email: bell.eapen@gulfdoctor.net; * Corresponding author

Abstract

Ultraviolet A photosensitivity is a debilitating symptom associated with the metabolic disorder Smith-Lemli-Opitz syndrome (SLOS). SLOS is a manifestation of the deficiency of 7-dehydrocholesterol reductase, an enzyme involved in the cholesterol biosynthesis. As a result several abnormal intermediary compounds are formed among which cholesta 5, 7, 9(11)-trien-3beta-ol is the most likely cause of photosensitivity. The effect of various drugs acting on cholesterol biosynthetic pathway on SLOS is not clear as clinical trials are not available for this rare disorder. A Flux Balance Analysis (FBA) has been carried out using the software CellNetAnalyzer or FluxAnalyzer to gain insight into the probable effects of various drugs acting on cholesterol biosynthetic pathway on photosensitivity in SLOS. The model consisted of 44 metabolites and 40 reactions. The formation flux of cholesta 5, 7, 9(11) - trien-3beta-ol increased in SLOS and remained unchanged on simulation of the effect of miconazole and SR31747. However zaragozic acid can potentially reduce the flux through the entire pathway. FBA predicts zaragozic acid along with cholesterol supplementation as an effective treatment for photosensitivity in SLOS.

Keywords: flux balance analysis; Smith-Lemli-Opitz syndrome

Background:

The Smith-Lemli-Opitz syndrome (SLOS) is a rare autosomal recessive disorder characterised by multiple congenital abnormalities. [1, 2] SLOS is a manifestation of an abnormality in the late phase of cholesterol biosynthesis due to an inherited deficiency of the enzyme 7-dehydrocholesterol-reductase [3]. It is caused by mutations in the DHCR7 gene coding for 7-dehydrocholesterol-reductase. [4]

As cholesterol is an important cell membrane constituent and a precursor of several important hormones, the clinical expression is diverse, ranging from facial dismorphism to limb and major organ defects. [3] However dermatologists are especially interested in the photosensitivity associated with SLOS which was unfortunately missed in the early reports of this syndrome. The first detailed report of photosensitivity occurred only in 1998 [5] and SLOS is now considered as the primary inherited photosensitivity syndrome with photosensitivity to Ultraviolet A. [6] The pattern of photosensitivity is also quite distinct with onset within minutes of sun exposure, sunburn-like erythema lasting for 24-36 hours and an action spectrum with a peak at 350 nm. [7]

Though the final stages of cholesterol biosynthesis are adequately described [8], the metabolic fate of 7-dehydrocholesterol (7-DHC) which accumulates as a result of the deficiency of its reductase enzyme in SLOS is unclear. Major C27 sterols observed in SLOS patients apart from cholesterol and 7-DHC are 8-dehydrocholesterol (8-DHC) and cholesta-5,7,9(11)-trien-3β-ol. [9] Cholesta-5,7,9(11)-trien-3β-ol is formed by oxidation of 7-DHC [10] and 8-DHC is formed by reverse isomerization of 7-DHC at the Δ5,7 level. [11] There has also been a report of the presence of an aromatic triene, 19-nor-5,7,9(10)-cholesta-trien-3β-ol [12] which can be considered an artefact. [9] It has recently been proved that among these aberrant metabolites, Cholesta-5,7,9(11)-trien-3β-ol is the most likely cause of Ultraviolet A photosensitivity. [1] Hence UVA photosensitivity is a symptom not directly related to deficiency of cholesterol.

Though cholesterol supplementation is found to be useful in relieving photosensitivity [6], the effect of other drugs which act on the final phase of cholesterol biosynthesis on this symptom is unknown. Among the several computational methods available for metabolic simulation, Flux Balance Analysis (FBA) will be appropriate for modelling this pathway as the detailed kinetic information is not available for all enzymes involved and more than one pathway exist to transform precursors to cholesterol [13] though it has traditionally been used to quantitatively simulate microbial metabolism. [14] FBA involves prediction of metabolic flux distribution based on stoichiometric, thermodynamic and reaction capacity constraints. FBA has been used here to understand the behaviour of the final stages of cholesterol biosynthesis in normal and SLOS individuals and to gain insight into the probable effects of drugs acting on this pathway on the symptom of photosensitivity.

Methodology:

FBA is a stoichiometric analysis technique used to model cellular behaviour in the absence of detailed kinetic information. [13] It is also useful in situations where an optimal flux distribution analysis is enough to generate quantitative hypotheses that may be tested experimentally as in SLOS.

A model of the final stages of cholesterol biosynthesis from the condensation of two molecules of farnesyl pyrophosphate onwards was prepared using

CellNetAnalyzer / FluxAnalyzer. **[15]** It is a MATLAB ® package for interactive network analysis.

The first nine reactions of cholesterol biosynthesis encompasses the mevalonate pathway which is common for several classes of compounds in addition to cholesterol. **[16]** The mevalonate pathway is highly regulated especially by feedback inhibition of HMG-CoA reductase by cholesterol and 7 DHC **[17]**. FBA is essentially an analysis of steady state and cannot adequately represent a feedback regulated or shared network. Hence these reactions were excluded from the model.

7-DHC has four metabolic fates apart from its conversion to cholesterol. Conversion to Vitamin D in the skin **[18]**, Isomerization to 8-DHC **[11]**, Oxidation to cholesta-5,7,9(11)-trien-3β-ol **[10]** and 19-nor-5,7,9(10)-cholesta-trien-3β-ol **[12]**. The flux through the formation of cholesta-5,7,9(11)-trien-3β-ol is important for photosensitivity.

The Biocyc repository of pathway models **[19]** provided the basic framework for the model. The metabolites and reactions are represented in Table 1 and Table 2 respectively (supplementary material). The minimum reaction rate is set to 0 for irreversible reactions and -1 for reversible reactions. The maximum rate was set to unity for all reactions, so that the model will provide the relative ratios of fluxes. The coefficient of objective function was also set to zero.

The imposition of these constraints resulted in a bounded solution space wherein every possible flux distribution must lie and an optimal metabolic flux distribution was calculated by the software using linear programming.

The loss of gene function in SLOS and enzyme inhibition by drugs are simulated by restricting the maximum flux through a particular reaction to a small value of 0.01. The flux through the input arm of the model (R1) was kept at the maximum possible value of one except for drugs blocking squalene synthase (R2) as the model will not be feasible. 19-nor-5,7,9(10)-cholesta-trien-3β-ol is now considered an artifact in fractions containing 8-dehydrocholesterol. **[9]** Hence the maximum flux through R36 which represents the formation of 19-nor-5,7,9(10)-cholesta-trien-3β-ol was also set to 0.01.

The effects of four groups of drugs were modelled. AY9944 and BM15766 class of compounds acting on 7-dehydrocholesterol reductase **[20]** thereby simulating SLOS (R22 and R26), Miconazole and related compounds acting on 14-α demethylase **[21]** in SLOS patients (R5 + R22 and R26), zaragozic acid and related compounds **[22]** interfering with Squalene Synthase (R2 + R22 and R26) and SR31747 group of compounds **[23]** inhibiting Δ8-Δ7 sterol isomerase (R39 + R22 and R26).

The optimal flux distribution was calculated after simulating the effect of each drug as mentioned above and the flux through the formation of cholesta-5,7,9(11)-trien-3β-ol which is important in photosensitivity was compared.

Results:
The model of the final phase of cholesterol synthesis built consisted of 44 metabolites (Table 1 in supplementary material) and 40 reactions (Table 2 in supplementary material). The relative flux distribution of the model is shown in (Figure 1). The flux through R 37 which represents the formation of cholesta-5,7,9(11)-trien-3β-ol will be indicative of the severity of photosensitivity. The inhibition of R22 and R26 as in SLOS resulted in doubling of flux through R37 from 0.2 to 0.49. There was no apparent change after blockage of R5 and R39 which simulates miconazole and SR31747 administration. However inhibition of R2 as in zaragozic acid administration resulted in the decline of flux through the entire pathway including R37 to almost zero.

Discussion:
The UVA photosensitivity in SLOS could be severe in some patients and the first detailed description of SLOS associated photosensitivity in a five-year-old girl describes how her parents tried to protect her from light by making a one-piece photoprotection suit with small openings for the eyes and mouth. **[5]** However there are not many studies on the management of this symptom even at this time.
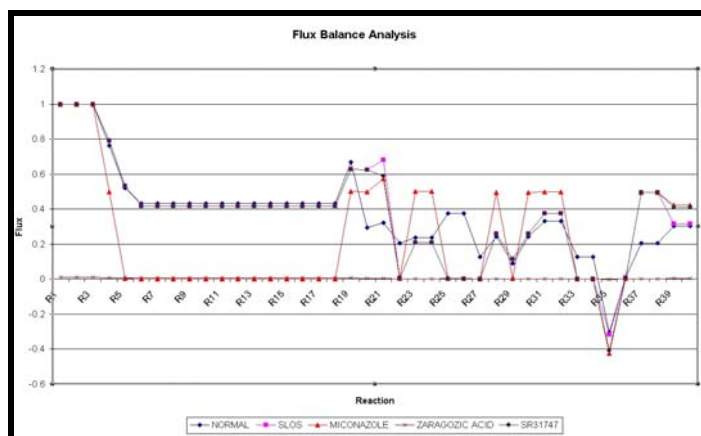
The first clinical trial on SLOS patients was for cholesterol supplementation and reported only subjective improvement in photosensitivity **[24]** which was corroborated by another study. **[25]** Though HMG-CoA inhibitor simvastatin along with cholesterol supplementation suppresses most of the symptoms of SLOS **[26]** there is no specific mention of its effect in photosensitivity except for a remark in a review. **[6]** Though the effect of feedback control of cholesterol on HMG-CoA reductase and the inhibition of the same enzyme by simvastatin is not directly apparent from our model, both can potentially reduce the flux through the input arm of the model (R1) thereby reducing the overall flux.

As per the model, the flux through R5 (14α-demethylation) is much greater than R28 (anaerobic reduction involving Δ24-reductase) which has the support of experimental evidence **[21]**. Miconazole and ketoconazole are frequently used azole antifungals, which inhibit the 14α-methyl demethylase enzyme, catalysing the preferred route for conversion of lanosterol to cholesterol. However there is no significant effect for these drugs on the terminal pathway as the alternate route involving Δ24-reductase gets activated. **[21]**

SR31747 is a novel immunosuppressive agent and an inhibitor of Δ8-Δ7 sterol isomerase. Tamoxifen is a commonly used antiestrogen inhibiting the same enzyme. The effects of both this drugs were simulated by blocking the reversible reaction (R39) which did not alter the flux distribution.

Zaragozic acid is a naturally occurring squalene synthase inhibitor, which has attracted attention because of its cholesterol lowering properties. **[22]** As this compound acts on R2, before the beginning of alternate pathways, it can potentially reduce the flux through the entire network including C37 important for photosensitivity. Hence zaragozic acid derivatives along with cholesterol

supplementation could be very effective in the management of photosensitivity in SLOS.

Figure 1: Relative flux distribution

Conclusion:

FBA has been used for several years to study cellular metabolism with high network connectivity and redundancy. It has also been used previously to identify probable drug targets. **[27]** This study demonstrates its use in the analysis of the effect of various drugs on an individual symptom of a metabolic disorder. Though reliability of FBA for a specific pathway is debatable, it provides some insight into the possible effect of certain well known drugs on photosensitivity, which needs to be clinically verified.

Resources:

The model prepared in CellNetAnalyzer is available from **[28].** Other resources including the model in SBML format and the reactions as a flat file are available from **[29]**.

References:
- **[01]** C. F. Chignell, *et al.*, *Free Radic Biol Med.*, 41: 339 (2006) [PMID: 16814115]
- **[02]** D. W. Smith, *et al.*, *J Pediatr.*, 64: 210 (1964) [PMID: 14119520]
- **[03]** G. Salen, *et al.*, *J Lipid Res.,* 37: 1169 (1996) [PMID: 8808751]
- **[04]** M. Witsch Baumgartner, *et al.*, *Hum Mutat.*, 17: 172 (2001) [PMID: 11241839]
- **[05]** C. R. Charman, *et al.*, *Br J Dermatol.*, 138: 885 (1998) [PMID: 9666840]
- **[06]** A. V. Anstey, *J Photochem Photobiol B.,* 62: 123 (2001) [PMID: 11566274]
- **[07]** A. V. Anstey, *et al.*, *Br J Dermatol.,* 141: 406 (1999) [PMID: 10583043]
- **[08]** J. L. Gaylor, *Biochem Biophys Res Commun.*, 292: 1139 (2002) [PMID: 11969204]
- **[09]** B. Ruan, *et al.*, *J Lipid Res.,* 42: 799 (2001) [PMID: 11352988]
- **[10]** E. De Fabiani, *et al.*, *J Lipid Res.*, 37: 2280 (1996) [PMID: 8978479]
- **[11]** A. K. Batta, *et al.*, *J Lipid Res.*, 36: 705 (1995) [PMID: 7616117]
- **[12]** A. K. Batta, *et al.*, *J Lipid Res.*, 36: 2413 (1995) [PMID: 8656079]
- **[13]** J. S. Edwards, *et al.*, *Environ Microbiol.*, 4: 133 (2002) [PMID: 12000313]
- **[14]** K. J. Kauffman, *et al.*, *Curr Opin Biotechnol.*, 14: 491 (2003) [PMID: 14580578]
- **[15]** S. Klamt, *et al.*, *Bioinformatics,* 19: 261 (2003) [PMID: 12538248]
- **[16]** P. Romero, *et al.*, Genome Biol., 6: R2 (2005) [PMID: 15642094]
- **[17]** J. L. Goldstein, *et al.*, Nature, 343: 425 (1990) [PMID: 1967820]
- **[18]** M. Rossi, *et al.*, *J Inherit Metab Dis.,* 28: 69 (2005) [PMID: 15702407]
- **[19]** P. D. Karp, *et al.*, *Nucleic Acids Res.*, 33: 6083 (2005) [PMID: 16246909]
- **[20]** M. Kolf Clauw, *et al.*, *Teratology*, 54: 115 (1996) [PMID: 8987154]
- **[21]** S. H. Bae, *et al.*, *Biochem J.,* 326: 609 (1997) [PMID: 9291139]
- **[22]** S. Nakamura, *Chem Pharm Bull,* 53: 1 (2005) [PMID: 15635219]
- **[23]** R. Paul, *et al.*, *J Pharmacol Exp Ther.,* 285: 1296 (1998) [PMID: 9618436]
- **[24]** M. Irons, *et al.*, *Am J Med Genet.,* 68: 311 (1997) [PMID: 9024565]
- **[25]** R. M. Azurdia, *et al.*, *Br J Dermatol.*, 144: 143 (2001) [PMID: 11167696]
- **[26]** P. E. Jira, *et al.*, *J Lipid Res.*, 41: 1339 (2000) [PMID: 10946022]
- **[27]** K. Raman, *et al.*, *PLoS Comput Biol.*, 1: e46 (2005) [PMID: 16261191]
- **[28]** http://www.gulfdoctor.net/bioinf/slos.zip
- **[29]** http://www.gulfdoctor.net/bioinf/slos.htm

Supplementary material

SQ	squalene
ESQ	2,3-Epoxysqualene
H_2O	Water
O_2	Oxygen
NADP	NADP
NADPH	NADPH
FORMATE	FORMATE
CO_2	Carbon Dioxide
LA	Lanosterol
C_8_24_DIEN	4,4-dimethyl-14a-hydroxymethyl-5a-cholesta-0,24-dien-3b-ol
F_C_8_24_DIEN	4,4-dimethyl-14a-formyl-5a-cholesta-8,24-dien-3b-ol
C_8_14_24_TRIEN	4,4-dimethyl-5-a-cholesta-8,14,24-trien-3-b-ol
C5_8_24_DIEN	4,4-dimethyl-5a-cholesta-8,24-dien-3-b-ol
HMC_8_24_DIEN	4a-hydroxymethyl-4b-methyl-5a-cholesta-8,24-dien-3b-ol
FMC_8_24_DIEN	4a-fonnyl-4b-methyl-5a-cholesta-8,24-dien-3b-ol
CMC_8_24_DIEN	4a-carboxy-4b-methyl-5a-cholesta-8,24-dien-3b-ol
MC_8_24_DIEN_ON	4a-methyl-5a-cholesta-8,24-dien-3-one
MZ	4-a-methyl-zymosterol
MC4_8_24_DIEN	4a-hydroxymethyl-5a-cholesta-8,24-dien-3b-ol
FC_8_24_DIEN	4a-formyl-5a-cholesta-8,24-dien-3b-ol
CC_8_24_DIEN	4a-carboxy-5a-cholesta-8,24-dien-3b-ol
C5_8_24_DIEN_ON	5a-cholesta-8,24-dien-3-one
Z	zymosterol
C_7_24_DIEN	5a-cholesta-7,24-dien-3b-ol
L	lathosterol
DHC7	7-dehydro-cholesterol
C	cholesterol
CYA	cycloartenol
DHD7	7-dehydro-desmosterol
D	desmosterol
DHL	24,25-dihydro-lanosterol
EN_8	4-a-methylcholesta-8-en-3b-ol
M	mestenol
E	Ergosterol
P	Phytosterol
DHC8	8-dehydro-cholesterol
EN8OL	cholesta-8-en-3b-ol
TRIEN_11	D-5,7,9(11)-trien
H2O2	Hydrogen Peroxide
NOR_10_19	d5,7,9(10)trien-nor
VITD3	vitd3
FDP	2-trans,trans-farnesyl-diphosphate
PSQ	presqualene-diphosphate
DIPHOSPHATE	diphosphate

Table 1: List of metabolites in the model

R1	2 FDP ==> PSQ + DIPHOSPHATE
R2	NADPH + PSQ ==> SQ + NADP + DIPHOSPHATE
R3	SQ + O2 + NADPH ==> ESQ + H2O + NADP
R4	ESQ ==> LA
R5	O2 + NADPH + LA ==> H2O + NADP + C_8_24_DIEN
R6	O2 + NADPH + C_8_24_DIEN ==> 2 H2O + NADP + F_C_8_24_DIEN
R7	O2 + NADPH + F_C_8_24_DIEN ==> H2O + NADP + FORMATE + C_8_14_24_TRIEN
R8	NADPH + C_8_14_24_TRIEN ==> NADP + C5_8_24_DIEN
R9	O2 + NADPH + C5_8_24_DIEN ==> H2O + NADP + HMC_8_24_DIEN
R10	O2 + NADPH + HMC_8_24_DIEN ==> 2 H2O + NADP + FMC_8_24_DIEN
R11	O2 + NADPH + FMC_8_24_DIEN ==> H2O + NADP + CMC_8_24_DIEN
R12	NADP + CMC_8_24_DIEN ==> NADPH + CO2 + MC_8_24_DIEN_ON
R13	NADPH + MC_8_24_DIEN_ON ==> NADP + MZ
R14	O2 + NADPH + MZ ==> H2O + NADP + MC4_8_24_DIEN
R15	O2 + NADPH + MC4_8_24_DIEN ==> 2 H2O + NADP + FC_8_24_DIEN
R16	O2 + NADPH + FC_8_24_DIEN ==> H2O + NADP + CC_8_24_DIEN
R17	NADP + CC_8_24_DIEN ==> NADPH + CO2 + C5_8_24_DIEN_ON
R18	NADPH + C5_8_24_DIEN_ON ==> NADP + Z
R19	Z ==> C_7_24_DIEN
R20	NADPH + C_7_24_DIEN ==> NADP + L
R21	O2 + NADPH + L ==> H2O + NADP + DHC7
R22	NADPH + DHC7 ==> NADP + C
R23	ESQ ==> CYA
R24	CYA ==> Z
R25	C_7_24_DIEN ==> DHD7
R26	DHD7 ==> D
R27	D ==> C
R28	LA ==> DHL
R29	C_8_24_DIEN ==> EN_8
R30	DHL ==> EN_8
R31	EN_8 ==> M
R32	M ==> L
R33	D ==> E
R34	D ==> P
R35	DHC7 <==> DHC8
R36	DHC7 ==> NOR_10_19
R37	O2 + DHC7 ==> TRIEN_11 + H2O2
R38	DHC7 ==> VITD3
R39	L <==> EN8OL
R40	EN8OL ==> DHC8

Table 2: List of reactions in the model